An Explanation of the Physical Origin of the Extra-ordinary Angular Tolerance of Cavity Resonator Integrated Grating Filters

Nadège Rassem, Anne-Laure Fehrembach and Evgeni Popov
Université d'Aix-Marseille, CNRS, Centrale Marseille, Institut Fresnel, Marseille, France

Keywords: Gratings, Subwavelength Structures, Bragg Reflectors, Eigenvalues, Resonance Domain.

Abstract: Cavity – resonator - integrated guided - mode resonance filters (CRIGFs) are promising structures that afford a very fine spectral width less than 1 nm. We study another structure to compare compare it to CRIGF. The angular acceptance of CRIGF is an order of magnitude greater than in classical gratings, even with complex pattern. To identify the phenomenon responsible for the extraordinary large angular acceptance of CRIGF, we study the dispersion curve of the mode excited in the CRIGF.

1 INTRODUCTION

With the increase of applications requiring spectral filtering, free space optical filters are the focus of several studies.

Fabry-Perot multilayer filters are the most widely used free space filters but show limits for narrow band filtering. To get a narrow spectral width with this type of filters, one needs a large number of layers thus increasing the size of the component which becomes unstable over time and with temperature.

Resonant grating filters are a very promising alternative relative to conventional multilayer filters. The resonant grating filter is composed of a stack of several dielectric layers on top of which a periodic nanostructure is engraved. The multilayer stack plays the role of a planar waveguide and the engraved structure allows to couple and decouple one eigenmode of the structure to the incident wave through one diffraction order of the grating. When the component is illuminated, a resonance peak occurs in the reflectivity or transmittivity spectrum. The characteristics of the peak, namely the centering wavelength and width, are mainly governed by the grating parameters. Those resonant grating structures are commonly called GMRF (Guided-mode Resonance Filters) and are known to have a very small angular tolerance. However they have a high quality factor and a very high rate of rejection.

The small angular tolerance is observed especially when the GMRF is illuminated under oblique incidence. That is to say when one single mode is excited through one diffraction order, usually the first order. In this configuration, it is possible to show (Evenor et al., 2012).

The spectral and angular width depends on the same parameters of the grating, namely the height h of the grating and its 1st Fourier coefficient. A small angular tolerance leads up to the degradation of the rate of rejection and to the spreading of the spectrum when the grating is illuminated with a beam with a large divergence. But if our grating is illuminated under normal incidence, two counter propagating modes are excited. In this configuration, the angular width depends on the 2nd Fourier coefficient while the spectral width depends on the first coefficient as shown in. (Evenor et al., 2012). Resonant grating filters with complex basic pattern have been proposed (Fehrembach et al., 2010), leading to an angular width of 0.5° at 1550nm for a bandwidth of 0.28nm. Yet, these record performance may be still insufficient for applications where the component have to be illuminated with a focused beam. In this optic another structure called CRIGF was introduced (X. Buet et al., 2012) and (K. Kintaka et al., 2012). It consists of a GMRF and a pair of distributed Bragg reflectors (DBRs) constructing a waveguide cavity resonator. We inserted a phase section between each DBR and the GMRF to optimize the reflectivity of the CRIGF.

Rassem N., Fehrembach A. and Popov E..
An Explanation of the Physical Origin of the Extra-ordinary Angular Tolerance of Cavity Resonator Integrated Grating Filters.

2 OBJECTIVES AND COMPARISION OF THE TWO STRUCTURES

The objective of our research is to improve the performances of resonant gratings. To begin, we compare two structures. The first component is periodic and is called “doubly periodic” structure (Figure 1). It is composed with a coupling grating (GMRF) and a Bragg grating with half filling factor and a period two times smaller than the GMRF grating. The two gratings are located one above the other. The second structure (Figure 2), called CRIGF (Cavity - Resonator -Integrated guided -mode-resonance filters), is non-periodic it is composed with one GMRF section and two Bragg reflector sections. The GMRF period is *d* and the DBR periods is *d*/2. The phase section is δ.

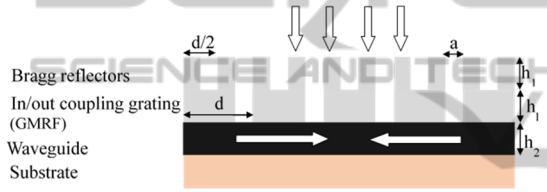

Figure 1: “doubly periodic" structure.

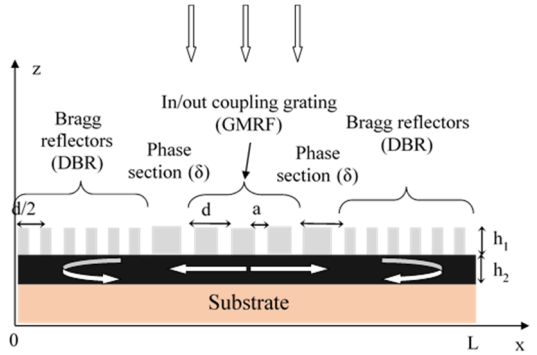

Figure 2: CRIGF structure.

The GMRF and the Bragg sections have both a groove width a = 100 nm and depth h_1 = 120 nm. The guiding layer thickness is h_2 = 165 nm. The indexes of the materials are 1.46 for the gratings and 1.97 for the guiding layer. The superstrate is air with index 1.0 (the same for the grating grooves) and the substrate is silica, with index 1.46. The period of the central section is d = 532 nm. The GMRF and Bragg reflectors included in the CRIGF have the same parameters than the “doubly periodic structure, and the phase section of the CRIGF is δ = 1.05d. The CRIGF is composed with 21 periods of GMRF and 200 periods.

Our aim is to compare the dispersion relations of the periodic and the non-periodic structures.

We plot on figure 3 the reflectivity versus the wavelength λ and the polar angle of incidence θ. The map shows a forbidden band, as it is well known for infinite resonant gratings. The reflectivity map is calculated for a planar incident wave. When a Gaussian beam is used, other calculations, not plotted here, show that the maximum of the reflectivity at resonance decreases with the size of the beam at waist when the beam divergence becomes too wide as compared to the angular tolerance of the component.

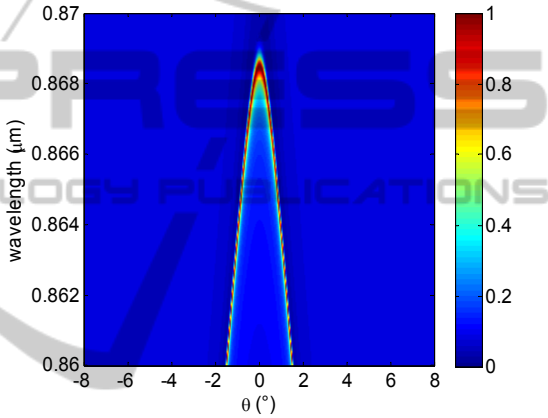

Figure 3: reflectivity of the "doubly periodic" with respect to the angle of incidence and wavelength, showing a forbidden band.

When we plot the reflectivity versus the wavelength λ and the polar angle of incidence θ for the CRIGF (figure 4), we observe a spot where the reflectivity is maximum. The spot is centered at λ = 864.9 nm and normal incidence. The incident beam is a Gaussian beam with a radius at waist of 5.2 µm, for which the maximum reflectivity at resonance is maximum (calculations not shown here).

This map is very different from that of the infinite grating plotted in figure 3. When the angle of incidence increases (in absolute value), or the wavelength moves away from 864.9 nm, the reflected energy decreases: the resonance degrades. This device has a wide angular acceptance, from -2° to 2°, together with a thin spectral width. The results of the calculations presented here were obtained using a home-made numerical code based on the Fourier Modal Method, also known as Rigorous Coupled Wave Analysis (RCWA), improved by using the more rapidly converging rules of factorization of

product of discontinuous functions enounced at (Li, 1997). The number of Fourier harmonics is truncated to from -700 to 700. To model a CRIGF with our RCWA code dedicated to model periodic structures, we use the so-called ”super-cell” method, which consists in considering the CRIGF as the basic pattern of a grating. For the modeling to be valid, it is necessary to isolate each basic cell from its neighbors. For this reason, the opportunity to add an absorbing layer between each basic cell is implemented. The absorbing layer consists of n_{slices} slices of homogeneous layers with a total thickness L_{ABS} and are characterized by an optical index n varying as $n(x) = n(x0) + i[(x - x0)/L_{ABS}]^2$, where x_0 is the x-starting position of the absorbing layer. The absorbing layer can be added inside the grating region, and waveguide region.

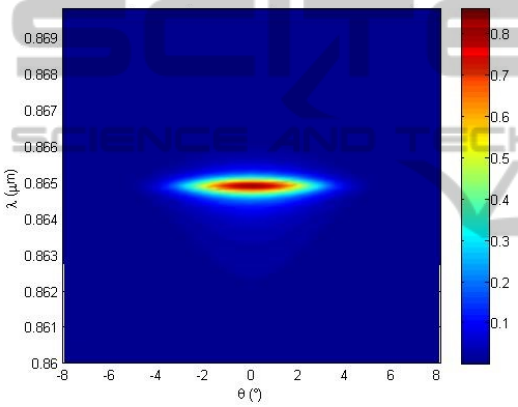

Figure 4: R (θ, λ) map of the CRIGF.

3 EIGENVALUES CALCULATION

To understand more the phenomenon presented on figure 4, we studied the behavior of the complex propagation constant of the excited eigenmode with respect to the angle of incidence, that is to say the dispersion relation. We employed the method described in ref. (Q. Cao et al., 2002). It consists in calculating the T-matrix of the structure from one edge to the other (from x=0 to x=L, see figure 2) The complex propagation constant g of the eigenmodes are related to the eigenvalues χ of the T matrix trough the relation:

$$\chi = \exp(i \gamma L) \quad (1)$$

L being the total length of the structure. For this calculation, the structure is repeated periodically along the z-direction, and we include absorbing layers between two adjacent structures. This configuration reduces the period of the problem considered for the numerical calculation and thus the truncation order of the Fourier series.

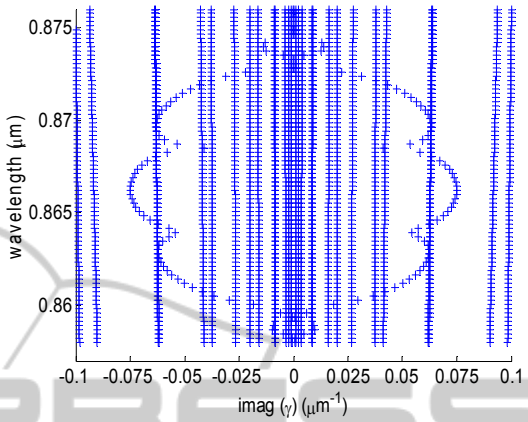

Figure 5: Imaginary parts of the propagation constants of the eigenmodes of the CRIGF with respect to the wavelength.

We plot in figure 5 the imaginary part of the propagation constants γ with respect to the wavelength. We can see many different eigenmodes with imaginary parts that depend quasi linearly on the wavelength and correspond to quasi-plane waves. Among these values, one eigenmode has a different behavior, showing an imaginary part that draws three major foils as a function of the wavelength. We identified the real part of the propagation constant of this different eigenmode. It is plotted on figure 6.

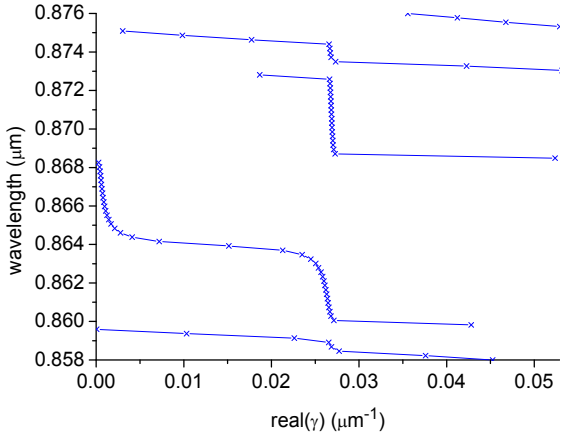

Figure 6: Real part of the propagation constant of the interesting eigenmode with respect to the wavelength.

This real part is characterized by a flat portion that appears around 864.9 nm, which corresponds to the center wavelength of the peak observed in Figure 4.

We note that from eq. 1, the real part of the eigenvalues is defined with an indetermination of 2 π / L = 0.0529 µm-1, L being the total length of the structure (L = 118.6892 µm).

Bellow, we study the evolution of the dispersion relations (the real and the imaginary part of γ) when introducing different strength of the Bragg reflectors, by varying the number of grooves of the Bragg grating. The central grating length is fixed constant, so that when varying the Bragg grating length, the length L_{nB} of the whole structure with varies.

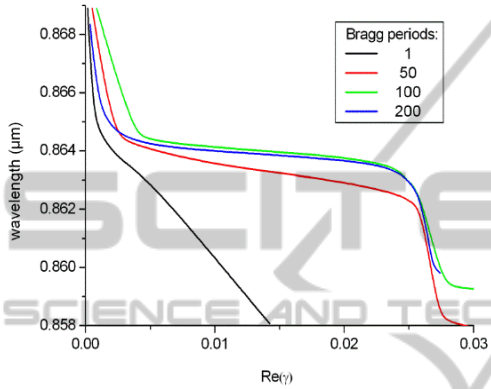

Figure 7: Evolution of the real part when varying the period of Bragg.

We present on fig. 7 the evolution of the "good" eigenvalues when the number of the Bragg grating periods increases from 1 to 200. As far as the values of real (γ) are determined within integer times 2π / L_{nB}, in order to avoid the change in this ambiguity, we plot the real part of γ L_{nB} / L with respect to the wavelength, where the total normalization length L = L_{200} = 118.6892 µm is kept fixed. We observe that the shape of the real part changes gradually with the DBR groove numbers, starting from the single-grating curve (calculated, without Bragg grating, but not shown here) towards the curve given in Figure 7. An increasingly flatter region is formed in the wavelength interval 0.863-0.865 µm.

In the following, we present an approached theory derived from the coupled-mode theory which allow to identify the physical origin of the extra-ordinary flattening of the dispersion curve.

Let us consider a grating waveguide, invariant in the y direction that supports leaky modes propagating in the x direction, with the leakage γ_{out} due to the radiation into a propagating diffraction orders in the substrate and the superstrate. The vector field components of the mode $F(x,z)$ can be factorized in the form:

$$F(x,z) = f(z)e^{ik_g x} \tag{2}$$

The propagation constant k_g is real without grating for waveguides made of lossless materials. For a grating waveguide, the radiation losses enter in the mode propagation constant along x and increase its imaginary part:

$$k_g = \mathrm{Re}(k_g) + i(\gamma_{out} + \gamma_{a.l.}) \tag{3}$$

with $\gamma_{a.l.}$ staying for the absorption losses, if any.

In addition to the leakage, the mode propagation constant and field map can be modified by the interaction between counter-propagating modes. The classical coupled-mode theory shows that this coupling modifies the propagation constant and forms a forbidden gap in its dispersion map; the modification resulting in a formation of two hybrid modes having two slightly different propagation constants (4):

$$\begin{aligned} k^+ &= K + \Delta \\ k^- &= K - \Delta \end{aligned} \tag{4}$$

with

$$\Delta = \sqrt{(K - k_g)^2 - \kappa^2} \tag{5}$$

κ is the coupling strength between the two counter-propagating modes and is proportional to the overlap mode integral in transverse direction. In particular, if the interaction involves the same counter-propagating modes and is due to the grating that extends from 0 to h in z-direction, then

$$\begin{aligned} \kappa &= \frac{\kappa_{-2}\kappa_{+2}}{4k_g^2} \\ \kappa_{\pm 2} &= k_0^2 \int_0^h F_{\pm 2}^T \left[n^2(x,z) \right] |f(z)|^2 \, dz \end{aligned} \tag{6}$$

and $F_m^T\left[n^2(x,z)\right]$ stays for the m-th Fourier transform, along x, of the square of the refractive index function of the grating.

The spectral region in which $|K - k_g| < \kappa$ is forbidden (band gap) in the sense that the imaginary part of the propagation constant increases due to the backward scattering. At its boundaries, the real part of $k^{\pm}$ has the weakest dependence on the incident vector component, parallel to the surface and thus the angular tolerances of the filter response are less tight.

Let us consider the CRIGF. To calculate his transmission matrix T_{total}, we need to express the transmission matrix of each Bragg grating, the transmission matrix of the GMRF (middle grating) and the transmission matrix at each interface Bragg/GMRF. We consider that we are at the boundary of the forbidden gap, so we have to take into account four modes with the propagation constants $+k^+$, $-k^+$, $+k^-$, $-k^-$ inside each region (Bragg grating and GMRF) (N. Rassem et al.).

We define for the Bragg grating and the GMRF, respectively the transmission matrix T_B and T_G.

T_B and T_G are expressed respectively as functions of $\pm k_B^{\pm}$, $\pm k_G^{\pm}$.

At the interfaces between the Bragg grating and GMRF, the interaction between the modes can be expressed through four overlap integrals (see ref. 5 for the full expressions): R^{++} for k_B^+ and k_G^+ , R^{--} for k_B^- and k_G^- , R^{+-} for k_B^+ and k_G^- , and R^{-+} for k_B^- and k_G^+..

We define an 8 x 8 transmission matrix R that contains the overlap integrals.

$$R = \begin{pmatrix} R^{++} & 0 & R^{-+} & 0 \\ 0 & R^{++} & 0 & R^{-+} \\ R^{+-} & 0 & R^{--} & 0 \\ 0 & R^{+-} & 0 & R^{--} \end{pmatrix} \quad (7)$$

The total transmission matrix is the product of the transmission matrices in the Bragg gratings T_B and the matrix containing the propagation in the middle grating T_G plus the interaction on the interfaces between the different gratings (R matrix):

$$T_{total} = T_B R^* T_G R T_B \quad (8)$$

In order to illustrate the influence of the mode interaction at the interface between the different gratings, in what follows we make several reasonable assumptions:

(1) Symmetrizing the problem by assuming that:

$$\begin{aligned} R^{++} &= R^{--} = R_1 \\ R^{-+} &= R^{+-} = R_2 \end{aligned} \quad (9)$$

We shall take these coefficients as real ($R_{1,2} \in Re$)

(2) Neglecting the radiation losses due to the transition effects on the interfaces between the gratings, and higher mode interactions. For this aim we consider the relation:

$$R_1^2 + R_2^2 = 1 \quad (10)$$

(3) Last, we assume that the Bragg gratings act as if localized on the interfaces x = 0 and L through the overlap integrals in R, i.e., considering the eigenvalues of $M = R^* T_G R$ instead of T_{total}.

To begin, we plot on figure 8 the evolution of the real part of the propagation constant with respect to the wavelength for several values of R^+-. We observe a behavior that is similar to that observed for the propagation constants calculated numerically (see figure 7). From these curves, we can conclude that the Bragg grating reflection plays a decisive role in the formation of the flat part in the dispersion curve, the stronger the coupling, the flatter the curve.

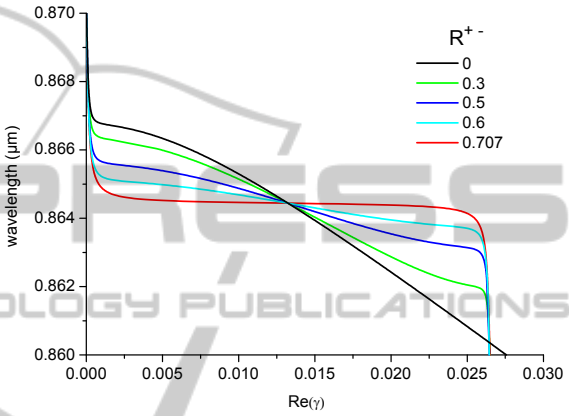

Figure 8: Evolution of the real part of the propagation constant for varying strength of coupling between the modes.

4 CONCLUSIONS

To sum up, we presented a study aiming at identifying the physical origin of the extra-ordinary flattening of the dispersion curve of CRIGF. We showed, both from a numerical study and from an approached model based on the coupled modes theory, that the dispersion curve flattening increases with the reflection on the Bragg grating. Moreover, the semi-analytical model allows us to attribute this extra-ordinary flattening of the dispersion curve to the coupling between modes that does not occur in infinite gratings. As it is well-known from the two-waves coupled mode theory, the interaction between two counter-propagative modes leads to a creation of two hybrid modes, one with a larger (k^+) and the other with a smaller (k^-) constant of propagation.

The Bragg grating cavity resonator that contains the central GMRF grating can leads to a well-known reflection of the mode "k^+" into the mode "$-k^+$" (and similarly for k^-), but also can provide an additional coupling between the hybrid modes ("k^+" into "$-k^-$") that does not exist without the Bragg grating box. We

have shown that the strength of this additional coupling (proportional to overlapping integral R^{-+}) is directly responsible for the flattening of the dispersion curve of the mode of the entire system. In particular, when the two types of coupling have similar strengths, one observes an extraordinary flattening of the dispersion curve of CRIGF devices.

In order to better understand how to improve the performance of this component (CRIGF), we plan to study the influence of each parameter of the structure.

REFERENCES

Evenor, I.; Grinvald, E.; Lenz, F. & Levit, S. *Analysis of light scattering off photonic crystal slabs in terms of Feshbach resonances* Eur. Phys. J. D., 2012, 66, 231-239.

Fehrembach, A.-L.; Lemarchand, F.; Talneau, A. & Sentenac, A. *High Q polarization independent guided-mode resonance filter with "doubly periodic" etched Ta2O5 bidimensional* grating *I.E.E.E. J. Light. Tech.,* 2010*, 28*, 2037-2044.

Q. Cao, Ph. Lalanne, and J.-P. Hugonin, "*Stable and efficient Bloch-mode computational method for one-dimensional grating waveguides,*" J. Opt. Soc. Am. 19, 335-338 (2002).

P. Paddon, and J. F. Young, "*Two-dimensional vector-coupled-mode theory for textured planar waveguides,*" Phys. Rev. B, 61, 2090 (2000).

N. Rassem, A.-L. Fehrembach, E. Popov "*Waveguide mode-in-the box with extra flat dispersion curve*", submitted JOSAA.

Li, L. "*New formulation of the Fourier modal method for crossed surface-relief gratings" J. Opt. Soc. Am. A,* 1997*, 14*, 2758-2767.

X. Buet, E. Daran, D. Belharet, F. Lozes-Dupuy, A. Monmayrant and O. Gauthier-Lafaye. "*High angular tolerance and reflectivity with narrow bandwidth cavity-resonator-integrated guided-mode resonance filter*". Optics Express, 20:9322-9327, 2012.

K. Kintaka, T. Majima, J. Inoue, K. Hatanaka, J. Nishii and S. Ura. *"Cavity-resonator-integrated guided-mode resonance filter for aperture miniaturization*". Optics Express, 20:1444-1449, 2012.